Multiple sources of passive stress relaxation in muscle fibres

Wolfgang A Linke and Mark C Leake[1]

Physiology and Biophysics Laboratory, University of Muenster, Schlossplatz 5,
D-48149 Muenster, Germany

E-mail: wlinke@uni-muenster.de

Abstract
The forces developed during stretch of nonactivated muscle consist of velocity-sensitive (viscous/viscoelastic) and velocity-insensitive (elastic) components. At the myofibrillar level, the elastic-force component has been described in terms of the entropic-spring properties of the giant protein titin, but entropic elasticity cannot account for viscoelastic properties, such as stress relaxation. Here we examine the contribution of titin to passive stress relaxation of isolated rat-cardiac myofibrils depleted of actin by gelsolin treatment. Monte Carlo simulations show that, up to ∼5 s after a stretch, the time course of stress relaxation can be described assuming unfolding of 1–2 immunoglobulin domains per titin molecule. For extended periods of stress relaxation, the simulations failed to correctly describe the myofibril data, suggesting that *in situ*, titin-Ig domains may be more stable than predicted in earlier single-molecule atomic-force-microscopy studies. The reasons behind this finding remain unknown; simply assuming a reduced unfolding probability of domains—an effect found here by AFM force spectroscopy on titin-Ig domains in the presence of a chaperone, alpha-B-crystallin—did not help correctly simulate the time course of stress relaxation. We conclude that myofibrillar stress relaxation likely has multiple sources. Evidence is provided that in intact myofibrils, an initial, rapid phase of stress relaxation results from viscous resistance due to the presence of actin filaments.

1. Introduction

Striated muscle often works under non-equilibrium conditions, i.e. consecutive stretches and releases prevent a skeletal or cardiac muscle from reaching a mechanical steady state.

[1] Present address: Clarendon Laboratory, University of Oxford, Parks Road, Oxford OX1 3PU, UK.
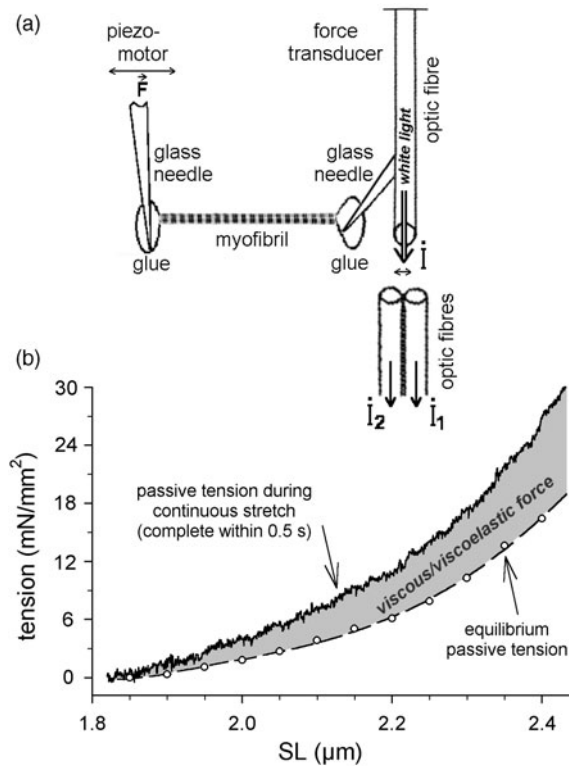
Figure 1. Force recordings on isolated myofibrils. (a) Schematic of the arrangement of optic-fibre based force transducer and piezomotor, with a myofibril (doublet) mounted. Force transducer calibration is done as described in Fearn *et al* (1993). (b) Passive sarcomere length-tension curves of a nonactivated rat cardiac myofibril. Passive tension at a given SL is higher during continuous stretch (solid curve) than in equilibrium (symbols and dashed curve; after stress relaxation). The difference is due to stretch speed-sensitive viscous/viscoelastic force components.

The stress experienced by a muscle is quite different in steady-state *versus* non-steady-state situations. For instance, when a nonactivated skeletal muscle (antagonist) is stretched by a contracting (agonist) muscle, the passive stress in the former increases but once the stretch stops (and the antagonist is held at a constant length), stress declines exponentially to approach a new quasi-steady-state level. This viscoelastic behaviour of nonactivated muscle is found also in isolated muscle fibres (Wang *et al* 1993, Anderson *et al* 2002) and even in a single isolated myofibril (Bartoo *et al* 1997). Figure 1 shows that the passive tension (PT) of an isolated myofibril is greater during continuous stretching than in equilibrium; the difference in PT is due to viscoelastic stress relaxation (figure 1(b)). Viscoelastic behaviour of nonactivated (passive) muscle samples manifests itself not only in stress relaxation (force decay at constant length), but also in creep (length increase at constant force following a stretch) and in hysteresis during a stretch-release cycle (Linke *et al* 1996a). The magnitude of the viscoelastic response correlates with the stretch/release rate (Bartoo *et al* 1997, Minajeva *et al* 2001). Also muscle length matters: at longer length the force-decay amplitude is higher, and stress relaxation lasts longer, than at shorter length (Minajeva *et al* 2001). These viscoelastic properties have long been known to be associated also with cardiac muscle (Noble 1977, Chiu *et al* 1982, de Tombe and ter Keurs 1992).
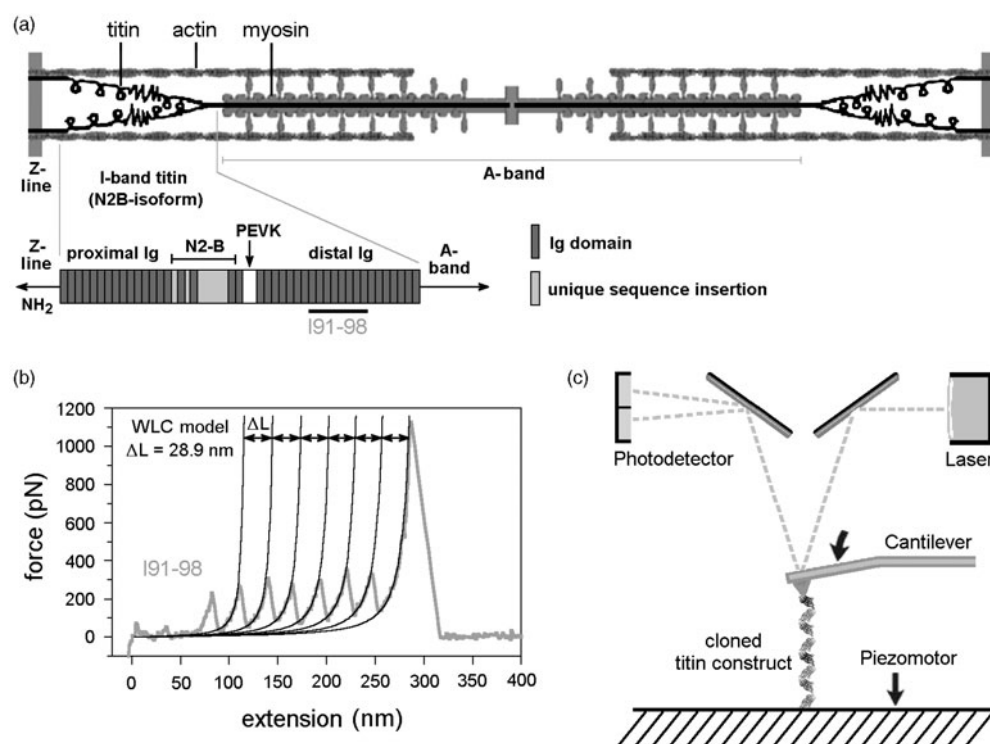
Figure 2. Atomic force microscopy (AFM) on titin domains. (a) Arrangement of titin in the sarcomere and domain structure of elastic I-band region of cardiac N2B-titin (after Labeit and Kolmerer (1995)). (b) Sawtooth pattern of the force-extension curve of I91–I98 (stretch rate, $1 \mu m \, s^{-1}$). Force peaks between 200 and 300 pN indicate Ig-domain unfolding events. Black lines are WLC fits to all peaks except the first. ΔL, contour length increment. (c) Principle of AFM method.

The molecular basis of viscoelasticity of passive muscle, such as stress relaxation, is not fully understood. 'Classical' representations portray viscoelasticity as a dashpot connected in series or in parallel to a spring (e.g., Maxwell or Voigt model, Fung (1993)). A different approach to elucidating passive viscoelasticity has been made possible over the past few years, as various methods of sub-cellular and molecular mechanics are available now to study directly the proteins potentially involved in determining viscoelastic behaviour. Recent attempts have been made to explain the viscoelasticity of passive muscle—at least at the fibre level—based on the molecular (mechanical) characteristics of the titin-filament system (Wang *et al* 1993, Higuchi 1996, Linke *et al* 1996a, Mutungi and Ranatunga 1996, Bartoo *et al* 1997, Minajeva *et al* 2001, Linke and Fernandez 2002, Opitz *et al* 2003, Trombitas *et al* 2003). Titins are a family of large elastic muscle proteins (molecular weight, 3000–3700 kDa) with a highly modular structure. A single titin molecule is $>1 \mu m$ long and consists of up to 300 domains of the immunoglobulin-like or fibronectin-like type, interspersed with unique sequences (Labeit and Kolmerer 1995). The molecule spans half of a sarcomere, the structural unit of skeletal and cardiac muscle (figure 2(a)), but only a segment of titin in the so-called I-band plays a role for muscular (visco)elasticity; the remainder of the molecule is firmly bound to other sarcomeric proteins and functionally inextensible (figure 2(a)). Recent evidence suggested that the steady-state (purely elastic) force component of a nonactivated myofibril can be reconstituted by using data obtained in single-molecule atomic-force microscopy

(AFM) force measurements on recombinant titin domains (Li *et al* 2002). In that study, the titin-based myofibrillar force was predicted with a three wormlike-chain (WLC) model of entropic elasticity fed with a plethora of single-molecule mechanical parameters. Although this approach is useful to reconstitute the steady-state elastic force of a myofibril, the WLC model cannot be used to explain stretch-velocity sensitive viscous/viscoelastic force components.

The question of how titin may contribute to muscle fibre viscoelasticity is the focus of this analysis. Specifically we asked whether titin itself, and/or interactions involving the elastic I-band titin (Kulke *et al* 2001, Linke *et al* 2002), could play a role in the viscoelastic force decay following stretch of myofibrils. We selected as our study object the isolated cardiac myofibril, since this preparation is readily accessible to various types of intervention, such as selective removal of actin filaments by gelsolin treatment (Linke *et al* 1997, Kulke *et al* 2001). In contrast, thin filaments are difficult or impossible to remove selectively from skeletal myofibrils (Minajeva *et al* 2002, Trombitas *et al* 2003). Extraction of actin filaments from myofibrils is useful for the present analysis, as in the actin-depleted sarcomere the titin-filament network is the only structure remaining in the I-band region of the sarcomere that extends during passive stretch. We tried to correlate the stress-relaxation characteristics measured in the actin-extracted cardiac myofibril with the molecular properties of titin domains, described using Monte Carlo (MC) simulations. The simulations again use data obtained by single-molecule AFM force spectroscopy (Carrion-Vazquez *et al* 1999, Marszalek *et al* 1999, Gao *et al* 2002, Li *et al* 2002, Watanabe *et al* 2002). In addition, here we apply AFM force spectroscopy on a recombinant titin construct to also provide evidence for an increase in the mechanical stability of titin-Ig domains in the presence of the small heat-shock protein, alpha-B-crystallin, an abundant chaperone in the cardiac cytoplasm which binds to I-band titin (Golenhofen *et al* 2002, Bullard *et al* 2004). Together the results indicate that the sources of myofibrillar stress relaxation are multifaceted, and may include titin-domain unfolding, as well as viscous resistance to stretch due to actin–titin interactions. Our findings also reveal that yet unknown factors appear to stabilize titin-Ig domains in the sarcomere, to prevent large-scale domain unfolding.

2. Experimental methods

2.1. Myofibril mechanics

Myofibrils were isolated from freshly excised rat cardiac muscle as described (Linke *et al* 1997). Briefly, thin muscle strips were dissected, tied to thin glass rods and skinned in buffer solution ('rigor', composed of (in mM): KCl 75, Tris 10, $MgCl_2$ 2, EGTA 2, pH 7.1) containing 0.5% Triton X-100 for $\geqslant$4 h. The skinned strips were homogenized in rigor buffer at 4 °C. A drop of the suspension was placed on a cover slip on the stage of an inverted microscope (Zeiss Axiovert 135). A myofibril was picked up with glass needle tips attached to a piezoelectric micromotor (Physik Instrumente, Karlsruhe, Germany) and a home-built force transducer with nanonewton sensitivity (figure 1(a)). To firmly anchor the specimen ends, the needle tips were coated with a water-curing silicone adhesive. Hydraulic micromanipulators (Narishige, Japan) were used to control the position of both needles. Experiments were performed in relaxing solution of 200 mM ionic strength, pH 7.1, at room temperature. Relaxing solution (for composition, see Linke *et al* (1997)) contained 20 mM 2,3-butanedione monoxime, an active-force inhibitor. All solutions were supplemented with the protease inhibitor leupeptin to minimize titin degradation (Linke *et al* 1998). To extract actin, a Ca^{2+}-independent gelsolin fragment (kindly provided by Dr H Hinssen) was added to the relaxing buffer at a final concentration of 0.2 mg ml^{-1}.

Force data collection and motor control were done with a PC, data acquisition board and custom-written LABVIEW software (Linke *et al* 1997, Kulke *et al* 2001). Sarcomere length (SL) was measured with a colour CCD camera (Sony), frame grabber, and Scion Image software (based on NIH image, Bethesda, MD). Force sampling rate was 5 kHz.

2.2. Atomic force microscopy (AFM) of cloned titin fragment I91–I98

The single-molecule AFM force-spectroscopy approach taken by us has been described (e.g., Carrion-Vazquez *et al* (1999), Li *et al* (2002)). The set-up is a homebuilt device that incorporates an AFM head stage purchased from Veeco Instruments (Mannheim, Germany). The experimental arrangement incorporating a Z-direction piezomotor (15 μm range, Physik Instrumente, Karlsruhe, Germany) is schematically shown in figure 2(c). The cantilevers of the force-measuring unit are standard Si_3N_4 cantilevers from Veeco Instruments. Cantilevers were calibrated in solution using the equipartition theorem. AFM experiments described were done with a cloned titin fragment containing eight different Ig domains, I91–I98 (figure 2(a), formerly I27–I34 (Li *et al* 2002)), according to the nomenclature of Freiburg *et al* (2000). The recombinant protein was a kind gift of Dr M Gautel.

In a typical AFM stretch experiment, protein sample concentrated at 0.17 μg ml^{-1} in phosphate-buffered saline (PBS, ionic strength 200 mM) was deposited onto a freshly evaporated gold coverslip and allowed to adsorb onto the surface. Five different motor stretch rates were applied, 200, 400, 1000, 1500 and 3000 nm s^{-1}. Figure 2(b) shows a representative force-extension curve of I91–I98 stretched at 1 μm s^{-1}. Seven sawtooth peaks (unfolding force, 200–300 pN) are seen, corresponding to the unfolding of seven Ig domains; the last peak at 1100 pN is reached when the protein detaches from the cantilever and/or cover glass. The force curves leading to each peak could be well described using the WLC model of entropic elasticity, which predicts the relationship between the relative extension of a polymer (z/L) and the entropic restoring force (f) through (Marko and Siggia 1995)

$$f = \left(\frac{k_B T}{A}\right)\left[\frac{1}{4(1 - z/L)^2} - \frac{1}{4} + \frac{z}{L}\right], \tag{1}$$

where k_B is the Boltzmann constant, T is the absolute temperature (here 300 K), A is the persistence length (a measure of the bending rigidity of the chain), z is the end-to-end length and L is the chain's contour length. The WLC model predicted that upon unfolding of each Ig domain, the contour length of the protein increases by 28.9 nm (figure 2(b)); this value is comparable to that found by others (e.g., Rief *et al* (1997), Li *et al* (2002)). We recorded the unfolding force level for each sawtooth peak and generated histograms for each stretch rate.

In another set of experiments, the construct I91–I98 was stretched in the presence of the chaperone alpha-B-crystallin, at a molar ratio of ∼130:1 (alpha-B-crystallin:titin). Here the protocol was to add 1 μl of 0.27 mg ml^{-1} alpha-B-crystallin to the (same) sample of titin and record force-extension curves again at the five different stretch rates. The calculated molar ratio follows from the M_w of 20.2 kDa for the former and ∼80 kDa for the latter, using 50 μl of 0.17 μg ml^{-1} I91–I98. Because some fraction of the alpha-B-crystallin molecules may bind to the gold, we estimated that the effective molar ratio of non-surface-bound alpha-B-crystallin to titin construct may be ∼70:1 (∼9 alpha-B-crystallin molecules per individual Ig domain), with an error of at least 20%. We thank Drs J Horwitz (Bova *et al* 1999) and B Bullard (Bullard *et al* 2004) for kindly providing recombinant alpha-B-crystallin. In control experiments, excess protein kinase A (catalytic subunit from bovine heart) was added to I91–I98 instead of alpha-B-crystallin; the effective molar ratio of protein kinase A to

I91–I98 was ∼60:1. In these experiments no change in the unfolding force of Ig domains was found.

2.3. Monte Carlo simulations

We attempted to reproduce the time course of stress relaxation after stretch of cardiac myofibrils by an MC technique based on entropic elasticity theory (WLC model) and the kinetic parameters of titin-Ig domain unfolding/refolding obtained in AFM stretch experiments with single titin polyproteins (Li *et al* 2002). Details of the MC approach used by us were described previously (Rief *et al* 1998). Here, the force decay following a stretch was assumed to be due to the unfolding of titin-Ig domains (Linke and Fernandez 2002). Refolding of domains was not considered in our calculations, as refolding has not been observed in the presence of a force (Oberhauser *et al* 1998, Carrion-Vazquez *et al* 1999). However, external force greatly affects domain unfolding. The probability of observing the unfolding of any module P_u was calculated as

$$P_u = \left(k_u^0 \Delta t\right)(\exp(f \Delta x_u / k_B T)), \tag{2}$$

where k_u^0 is the Ig-domain unfolding rate at zero force, Δt is the polling interval, f is applied force and Δx_u is the unfolding distance (Linke and Fernandez 2002). The simulations were performed in a LABVIEW (National Instruments, Austin, TX) software environment. A feature of the custom-written software allowed selection of a desired number of iterations.

3. Results and discussion

3.1. Time course of stress relaxation in isolated cardiac myofibrils

A possibility is that the phenomenon of myofibrillar viscoelasticity arises from the unfolding of a low number of Ig domains in titin (Minajeva *et al* 2001, Linke and Fernandez 2002). Step-wise force relaxation in titin molecules suggesting unfolding of individual domains has been observed in a single-molecule mechanics study using optical tweezers (Tskhovrebova *et al* 1997). Therefore, our approach was to try to reproduce the force response of nonactivated rat cardiac myofibrils to a stretch-hold protocol with an MC simulation that takes into account the entropic elasticity of titin (equation (1)) and the unfolding characteristics of Ig domains established by AFM work (Li *et al* 2002). This kind of analysis has been done previously on rabbit cardiac myofibrils but only over a limited stress-relaxation period of 5 s (Linke and Fernandez 2002). Here we extended the hold period to 20 s and, unlike in the earlier study, we used actin-extracted myofibrils to make sure there is no contribution to viscoelasticity due to the presence of muscle thin filaments.

The force data to be reproduced were obtained by extending rat cardiac myofibrils (diameter, ∼2 μm) in relaxing buffer in two quick steps (each 25 ms, corresponding to physiological rates of stretch) from slack length (∼1.9 μm SL) to 2.1 μm and 2.3 μm SL, respectively (figure 3). At the long SL, the sample was held for 20 s, before being released back to 2.1 μm SL and to slack length. After a rest period of 1 min the stretch-hold-release protocol was repeated up to 10 times and data were averaged to increase the signal-to-noise ratio. The force traces obtained from a given myofibril were found to be highly reproducible. Four different myofibrils were probed this way and force responses similar to that shown in figure 3(a) were obtained (for means and error estimates see figure 6).

In a next step, each myofibril was exposed to a Ca^{2+}-independent gelsolin fragment (concentration, 0.2 mg ml^{-1} relaxing buffer) for 4 min to remove actin filaments; actin extraction was routinely checked by staining with rhodamine-phalloidin (figure 3, right panels).
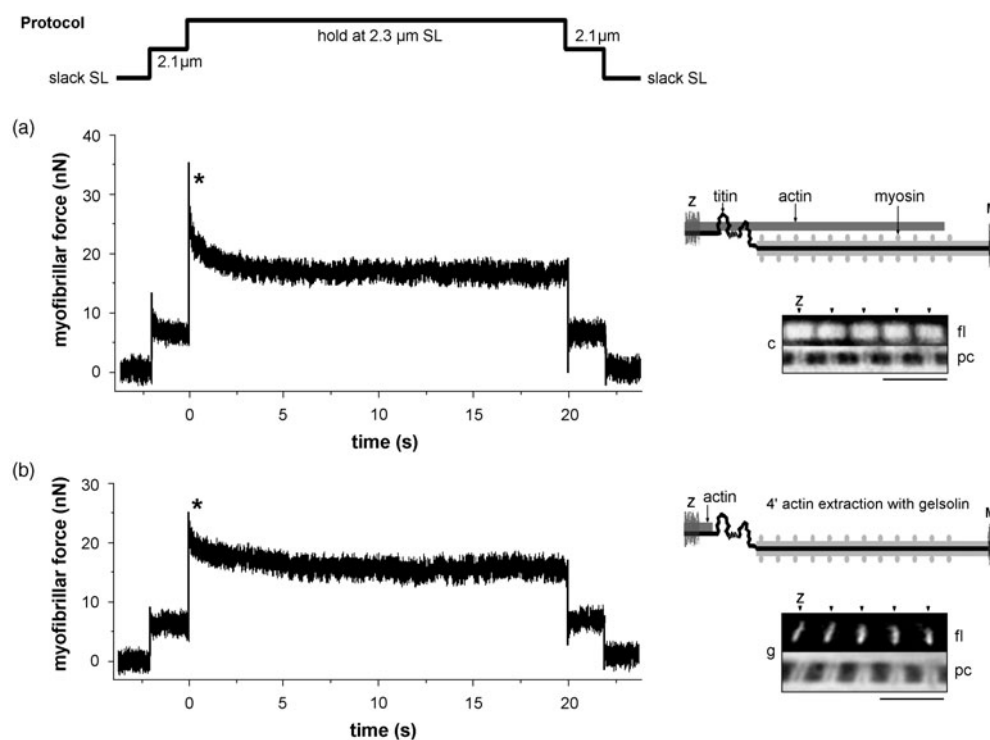
Figure 3. Stress relaxation of stretched nonactivated rat cardiac myofibril, before and after extraction by Ca^{2+}-independent gelsolin fragment. Top: stretch protocol. Stretch time, 25 ms. SL, sarcomere length. (a) Passive force response of non-extracted myofibril. (b) Passive force response of myofibril treated with Ca^{2+}-independent gelsolin fragment for 4 min to extract actin. Selective removal of actin filaments diminishes mainly the rapidly decaying viscous/viscoelastic force (asterisk), not the steady-state (elastic) force. Right panels in (a) and (b) explain the gelsolin effect. Photographs show fluorescence images (fl) of control (=c) and gelsolin-treated (=g) myofibrils stained with rhodamine-phalloidin to visualize actin, and corresponding phase-contrast (pc) image. Bars, 5 μm. Z, Z-line (and arrow heads).

In cardiac myocytes, thin filaments are rapidly removed by gelsolin, except the portion attached to titin in a 100-nm-wide region adjoining the Z-disc (figure 3(b), right panel; Granzier *et al* (1997), Linke *et al* (1997)). Analysis of stress relaxation before and after 4-min-gelsolin treatment showed a drop in peak-force amplitude by approximately one third (figures 3(a), (b)). Only the rapidly decaying force at the start of the hold period appeared to be reduced (asterisks in figures 3(a), (b)), not the slowly decaying force component. Elsewhere we provided evidence for weak binding between the I-band region of titin, specifically the PEVK domain, and actin filaments (Kulke *et al* 2001, Linke *et al* 2002), giving rise to viscous resistance to myofilament sliding (Opitz *et al* 2003). The present results confirm this notion: the reduction of rapidly decaying force, on actin extraction, likely reflects the removal of actin–titin interactions and the lowered viscous drag. In a thin-filament extracted sarcomere, the main (if not sole) structure connecting the Z-disc to the thick filaments should be the I-band titin (figure 3(b), right panel). Consequently, titin proteolysis by low doses of trypsin completely suppresses the passive force response of actin-extracted cardiac myofibrils to stretch (Kulke *et al* 2001). In the following, we use the stress-relaxation response after gelsolin treatment (figure 3(b)) as the reference force data that is tried to be reproduced by MC simulation.
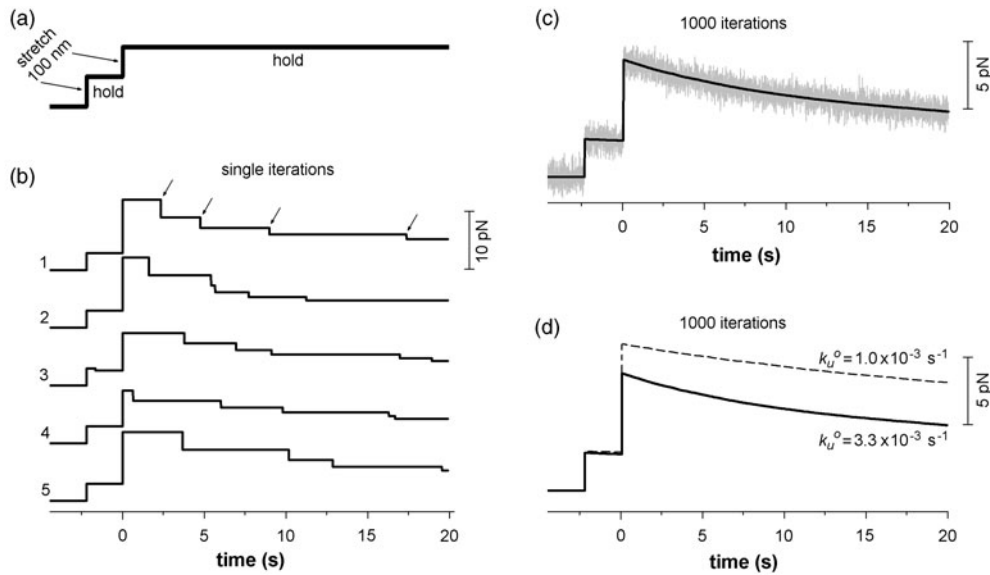
Figure 4. Monte Carlo simulation of force decay in stretched titin molecules due to Ig-domain unfolding. (a) Two 100 nm stretches are followed by hold periods, of which the second is 20 s long. (b) Five examples of single iterations. Arrows indicate Ig-domain unfolding event (drawn only for top trace). (c) Simulated force relaxation of N2B-cardiac titin assuming Ig-domain unfolding with $k_u^0 = 3.3 \times 10^{-3}$ s^{-1} (see equation (2)). Black solid line is average of 1000 iterations, grey shade is added white noise. (d) Simulated force relaxation (average of 1000 iterations) using the two different k_u^0 values indicated.

3.2. Monte Carlo simulation of viscoelastic force decay

In the MC simulations, we used the same parameters of titin-domain function as those used by Linke and Fernandez (2002), after Li *et al* (2002). Specifically, the unfolding rate at zero force, k_u^0, of the mechanically weakest Ig domain characterized so far by AFM work, is $\sim 3.3 \times 10^{-3}$ s^{-1} (the I4 domain of the proximal tandem-Ig segment; Li *et al* (2002)); we used this value to calculate the Ig-domain-unfolding probability, P_u (equation (2)). The modelling also considered the presence of the unique sequences in cardiac I-band titin (N2B-isoform; figure 2(a)), which are modelled as WLC springs with a combined contour length of 300 nm (PEVK = 70 nm; N2B unique sequence = 230 nm) and a persistence length of 0.9 nm (Li *et al* 2002). A fixed value in the simulation is the number of Ig domains within the extensible section of one titin molecule, which is 41 in the N2B-isoform of cardiac titin, the main isoform in rat heart (Freiburg *et al* 2000, Neagoe *et al* 2003, and figure 2(a)). For unfolding distance, we use a value of 0.25 nm and for the contour-length gain upon unfolding of one Ig domain, 28.5 nm (Carrion-Vazquez *et al* 1999).

Figure 4(b) shows single iterations of the MC-based force simulation, obtained by simulating the stretch-hold protocol illustrated in figure 4(a). The stretch amplitudes in the model are 100 nm for the initial step and another 100 nm for the second step, which reproduces the amount of stretch imposed onto I-band titin in sarcomeres extended by ΔSL = 0.2 μm from 1.9 and 2.1 μm SL, respectively. Here the focus was on the second step and the following hold period of 20 s. The five representative traces shown in figure 4(b) suggest that, over the 20-s-long hold period, 4 to 5 Ig domains per titin molecule unfold (arrows in top trace). The average force of 1000 iterations was calculated and white noise was

added to the force trace to make it look more 'real' (figure 4(c), solid line and grey shade). The simulated trace recovers the phenomenon of stress relaxation. As an average of 1000 iterations was calculated, the averaged force trace was essentially identical in different runs of the MC simulation.

The unfolding rate at zero force, k_u^0, has been found to vary significantly between different titin Ig domains (Li *et al* 2002). To test the effect of variations in k_u^0 on the calculated stress-relaxation trace, we changed the value of 3.3×10^{-3} s^{-1} used in the MC simulation of figure 4(c), to 1.0×10^{-3} s^{-1} in figure 4(d) (for rationale, see the next section). This modification increased the force after the second step and slightly affected the time course of stress relaxation over the 20-s-hold period (figure 4(d), dashed curve).

3.3. Modifications of titin Ig-domain stability measured by AFM force spectroscopy

The sensitivity of the MC simulation to variations in k_u^0 suggests that relatively minor modifications in Ig-domain stability could strongly affect the stress relaxation of a myofibril, if Ig-domain unfolding were indeed underlying the passive-force decay following stretch. In this context, evidence was put forth elsewhere indicating that titin Ig domains may be more stable in the natural environment of the sarcomere than in *in vitro* AFM force measurements (Trombitas *et al* 2003). If so, Ig domains could be stabilized in the myofibril by some factor(s) currently unknown. Aggregation of titin strands in the sarcomere (Liversage *et al* 2001, Tskhovrebova and Trinick 2003) is a possibility, whereas the stability of Ig domains does not seem to be affected by the presence of thin filaments (Trombitas *et al* 2003). However, one can envision many sarcomeric and/or non-sarcomeric proteins possibly interacting with I-band titin domains. Established interactions have been summarized in overview articles (Granzier and Labeit 2004, Miller *et al* 2004), but few proteins are known to bind to the functionally extensible titin Ig-domain region. A protein recently shown to associate with cardiac-titin Ig domains in the I-band is the small heat-shock protein, alpha-B-crystallin (Bullard *et al* 2004). Alpha-B-crystallin constitutes ∼3–5% of the total soluble protein content of cardiac muscle and it protects the myofibres from the effects of ischemia, preventing extensive structural damage (Golenhofen *et al* 2002). Here we wanted to test whether this chaperone has an effect on Ig-domain stability in AFM force measurements, speculating that the action of alpha-B-crystallin could be one of many natural ways how to modify the mechanical properties of an Ig domain. Hence, we performed single-molecule AFM force spectroscopy on a recombinant titin-Ig-domain construct, I91–I98 (figure 2(a)) and tested the effect of alpha-B-crystallin on its mechanical parameters.

Results are shown in figure 5. At the same stretch rate of ∼1 μm s^{-1}, the unfolding force level of individual Ig-domains in I91–I98 typically was higher in the presence of alpha-B-crystallin than in PBS alone (figure 5(a)), whereas ΔL (measured as in figure 2(b)) was unchanged. Histograms constructed for each dataset revealed that the mean unfolding force of I91–I98 domains in PBS is 244 pN—comparable to values reported elsewhere (e.g., Li *et al* (2002))—whereas that in PBS plus alpha-B-crystallin is 280 pN (figures 5(b), (c)). Similar analyses were done for different stretch rates and a plot of unfolding force *versus* $\log_{10}$ velocity was constructed (figure 5(d)). Error estimates are relatively high, because individual Ig domains in I91–I98 show quite different unfolding force levels (Li *et al* 2002). Elsewhere we showed that, if the forces in just the first and fourth peaks are compared, there is a statistically significant difference ($p < 0.05$ in Student's *t*-test) in unfolding force by 40–60 pN between PBS alone and PBS+alpha-B-crystallin, at a stretch rate of 1000 nm s^{-1} (Bullard *et al* 2004). From the linear fits to each dataset (figure 5(d)) we calculated (see Carrion-Vazquez *et al* (1999)) that k_u^0 in the presence of alpha-B-crystallin is smaller than that
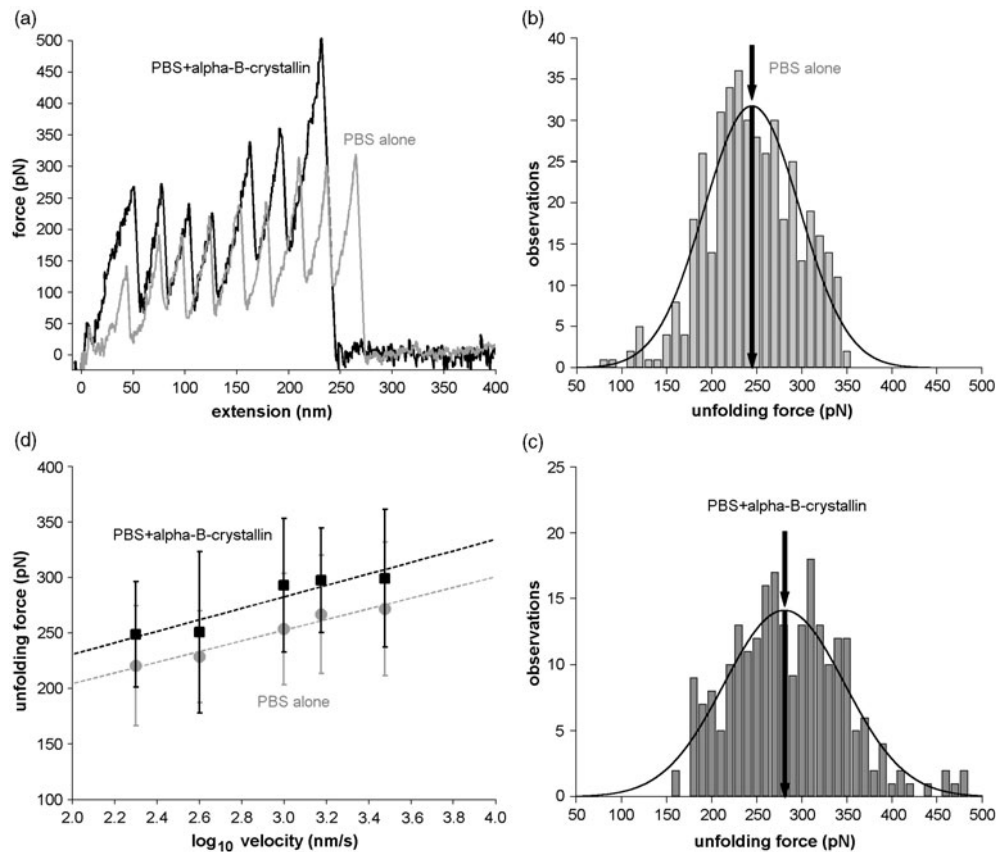
Figure 5. Effect of alpha-B-crystallin on Ig-domain stability, measured by AFM force spectroscopy on I91–I98 titin domains (cantilever stiffness, $\sim$40 pN nm^{-1}). (a) Original force-extension curves showing higher unfolding forces in the presence of alpha-B-crystallin, compared to PBS alone. Stretch rate, $\sim$1 μm s^{-1}. (b) Histogram and Gaussian distribution of unfolding forces measured at stretch rates of $\sim$1 μm s^{-1}, for I91–I98 in PBS. (c) Histogram and Gaussian distribution of unfolding forces measured at the same stretch rate, but with I91–I98 in PBS+alpha-B-crystallin. Note the increase in average unfolding force by $\sim$35 pN compared to (b). (d) Plot of unfolding force versus logarithm of stretch velocity, for five different stretch rates. Data are mean $\pm$ SD. Linear fits to each dataset are shown.

in PBS, by a factor of $\sim$3. Thus, the presence of alpha-B-crystallin substantially reduces the probability of unfolding, P_u, of Ig domains. However, future work is needed to determine how alpha-B-crystallin acts to mechanically stabilize Ig domains. The principal conclusion in the context of this study is that there are factors present in the cardiomyocyte which are capable of stabilizing titin-Ig domains.

3.4. Reconstitution of myofibrillar stress relaxation using MC simulations

We now wanted to compare the stress relaxation measured in actin-extracted cardiac myofibrils (figure 3) with that calculated in MC simulations (figure 4). Figure 6(a) illustrates the mean (black line) and SEM (grey shade) of force measurements on four different cardiac myofibrils. The results of the MC simulation are shown using a k_u^0 value of 3.3×10^{-3} s^{-1} (figure 6(b)) and
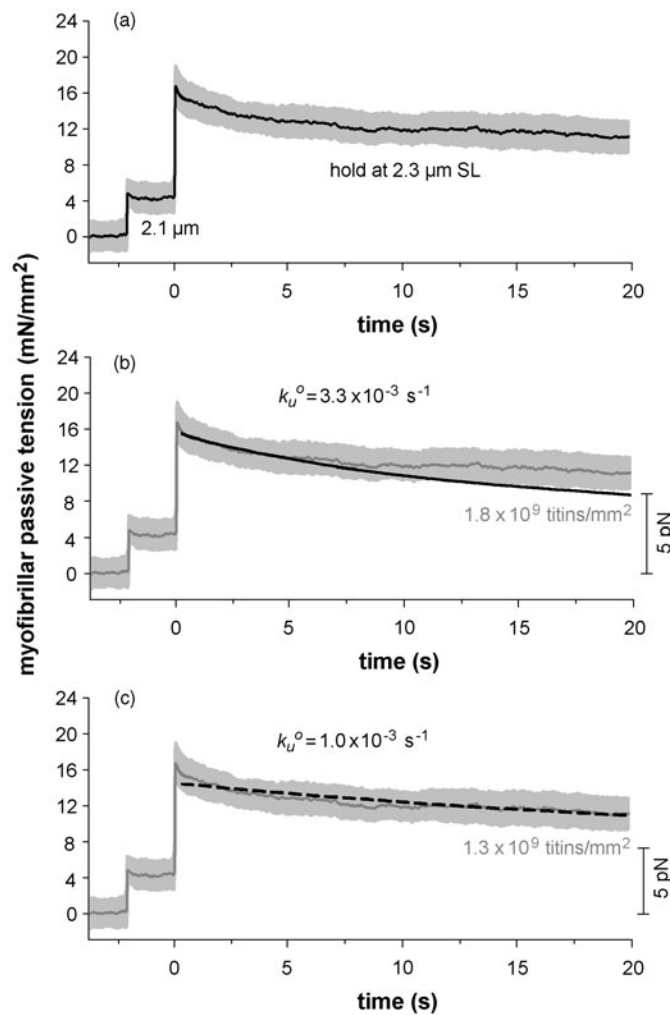
Figure 6. Comparison of MC simulation of 'stress relaxation' based on titin Ig-domain unfolding with stress relaxation of actin-extracted rat cardiac myofibrils. (a) Mean (black solid curve) $\pm$ SEM (grey shade) of passive tension of four rat cardiac myofibrils, stretched using the protocol shown in figure 3. (b) Monte Carlo simulation of 'stress relaxation' (black solid curve) using $k_u^0 = 3.3 \times 10^{-3}$ s^{-1} (1000 iterations) and a scaling factor of 1.8×10^9 titin molecules per mm^2, in comparison to mean (dark grey curve) and error (grey shade) of myofibrillar stress relaxation. The simulation recovers the time course of myofibrillar stress relaxation for the first $\sim$5 s only. (c) Monte Carlo simulation of 'stress relaxation' (black dashed curve) using $k_u^0 = 1.0 \times 10^{-3}$ s^{-1} (1000 iterations) and a scaling factor of 1.3×10^9 titin molecules per mm^2, in comparison to mean (dark grey curve) and error (grey shade) of myofibrillar stress relaxation. Compared to (b), k_u^0 is lowered by a factor of approximately three, mimicking the effect of alpha-B-crystallin on Ig-domain stability.

1.0×10^{-3} s^{-1} (figure 6(c)). In both panels the calculated force per single titin molecule was scaled up to the myofibril level by accounting for the number of titin strands per myofibrillar cross-sectional area: for best fits we used values of 1.8×10^9 (figure 6(b)) and 1.3×10^9 (figure 6(c)) titin molecules per mm^2. This compares to $\sim$2.4 $\times 10^9$ titins per mm^2 suggested by others (Higuchi *et al* 1993, Liversage *et al* 2001).

Using the higher value of $k_u^0 = 3.3 \times 10^{-3}\,\text{s}^{-1}$, the simulated trace followed the myofibril data for an initial ∼5 s of force relaxation, but then deviated significantly (figure 6(b)). This result confirms and extends our earlier notion (Linke and Fernandez 2002) of a similarity in the time course of slow stress relaxation measured and simulated over a period of 5 s. During this time period, 1–2 Ig domains per titin molecule would be predicted to unfold (figure 4(b)). This analysis now showed that the force decay in (actin-extracted) myofibrils levels out after 5 s, whereas the simulated force continues to decrease (figure 6(b), black line). Thus, in the environment of the sarcomere, titin-Ig domains appear to be more stable than predicted by AFM mechanical measurements. In agreement with Trombitas *et al* (2003), the apparently higher-than-expected stability of Ig domains is not related to the presence of actin filaments. Reason(s) for the less prominent stress relaxation of myofibrils, compared to the MC prediction, may include stabilization of Ig domains by interacting neighbouring titin molecules (Tskhovrebova and Trinick 2003)—the half-sarcomere of a myofibril contains 1000–2000 parallel titin molecules—and/or interaction of titin domains with other sarcomere proteins or soluble cytoplasmic proteins.

We then asked whether a decreased Ig-domain unfolding probability could help obtain a better match between myofibril data and MC simulations. The dashed curve in figure 6(c) was constructed using $k_u^0 = 1.0 \times 10^{-3}\,\text{s}^{-1}$, e.g., a reduction compared to figure 6(b) by a factor of approximately three. Although the simulated curve lies within the error estimates of the myofibril data, the shape of the calculated curve does not satisfactorily describe the mean time course of measured stress relaxation; the simulated curve does not follow the unique curvature of the measured data. Additionally, we needed to use a relatively low value of 1.3×10^9 titin molecules per mm^2 to scale up to the myofibril level, which is only approximately half the value suggested elsewhere (Higuchi *et al* 1993, Liversage *et al* 2001). These results indicate that using a lowered unfolding probability of Ig domains in the MC simulation is nevertheless insufficient to explain the myofibril data. Thus, although titin-Ig domain unfolding could still play a role for myofibrillar stress relaxation, it is clear that it cannot be the sole determinant of viscoelastic force decay and it is likely that other factors contribute to the phenomenon. We conclude that the use of mechanical parameters obtained in single-molecule titin AFM studies does not allow to faithfully reconstitute myofibrillar stress relaxation, even if one element contributing to viscosity/viscoelasticity, the thin filaments, is removed from the sarcomere.

4. Conclusions

The results of this study allow the following conclusions:

(1) The molecular origins of myofibrillar passive viscoelastic behaviour such as stress relaxation are most likely multifaceted. Unlike the elastic-force component of nonactivated cardiac myofibrils, which is explainable by the entropic-spring properties of serially connected titin segments (Li *et al* 2002), viscoelastic forces cannot be straightforwardly described by simple models fed with currently available single-molecule AFM data.

(2) Ig-domain unfolding could underlie part of the stress-relaxation phenomenon, but if so, only a very small number of Ig domains per titin molecule is predicted to unfold, in agreement with previous conclusions by Minajeva *et al* (2001) and Linke and Fernandez (2002). If unfolding did occur, it is predicted to take place in some proximal Ig domains of I-band titin, not the mechanically more stable distal domains (Li *et al* 2002).

(3) However, in the natural setting of the sarcomere, titin-Ig domains appear to be more stable than predicted by AFM mechanical measurements. This view is consistent with that of

Trombitas *et al* (2003). At this point we do not know what could cause the increased domain stability *in situ*. Simply assuming a reduced unfolding probability of domains—an effect observed here by AFM force spectroscopy on titin-Ig domains in the presence of a chaperone, alpha-B-crystallin—did not help recover the correct time course of stress relaxation of actin-depleted cardiac myofibrils.

(4) The fact that the time course of cardiac myofibrillar stress relaxation can nevertheless be correctly simulated based on measured Ig-domain unfolding parameters, for the first ~5 s after a stretch (Linke and Fernandez (2002), and figure 6(b)), may indicate that a few (1–2 Ig domains per titin molecule) do indeed unfold *in situ*, or it might just be coincidental.

(5) Then, other factors could add to the viscoelastic force decay. Possible sources in the sarcomere, which may potentially contribute to stress relaxation, are the Z-disc and the A-band, both serving as anchorage points for the elastic titin. Also, any sliding of large protein strands like titin or thick and thin filaments through a liquid will be accompanied by viscous effects (Opitz *et al* 2003), thus adding to global viscosity. Weak interactions between actin and myosin have been shown to make only a minor contribution to cardiac myofibrillar stress relaxation (Kulke *et al* 2001, Linke and Fernandez 2002).

(6) Another possibility is that also the unique intervening sequences in I-band titin, PEVK and/or N2-B, contribute (partly) to the stress relaxation. However, single-molecule mechanical studies have revealed conflicting results as to whether or not these sequences have the potential for such a contribution (Kellermayer *et al* 2001, Li *et al* 2002, Watanabe *et al* 2002). Further experimental studies are necessary to resolve this issue.

(7) The above points notwithstanding, and extending our earlier findings (Kulke *et al* 2001, Linke and Fernandez 2002), a large proportion of the passive-force decay can be ascribed to viscous drag due to the presence of actin filaments, in particular weak actin–titin interactions. These interactions manifest themselves in a quick force relaxation immediately following a stretch but also in viscous resistance to sarcomere shortening (Opitz *et al* 2003).

References

Anderson J, Joumaa V, Stevens L, Neagoe C, Li Z, Mounier Y, Linke W A and Goubel F 2002 Passive stiffness changes in soleus muscles from desmin knockout mice are not due to titin modifications *Pflügers Arch.* **444** 771–6

Bartoo M L, Linke W A and Pollack G H 1997 Basis of passive tension and stiffness in isolated rabbit myofibrils *Am. J. Physiol.* **273** C266–76

Bova M P, Yaron O, Huang Q, Ding L, Haley D A, Stewart P L and Horwitz J 1999 Mutation R120G in alphaB-crystallin, which is linked to a desmin-related myopathy, results in an irregular structure and defective chaperone-like function *Proc. Natl Acad. Sci. USA* **96** 6137–42

Bullard B *et al* 2004 Association of the chaperone alpha B-crystallin with titin in heart muscle *J. Biol. Chem.* **279** 7917–24

Carrion-Vazquez M, Oberhauser A F, Fowler S B, Marszalek P E, Broedel S E, Clarke J and Fernandez J M 1999 Mechanical and chemical unfolding of a single protein: a comparison *Proc. Natl Acad. Sci. USA* **96** 3694–9

Chiu Y L, Ballou E W and Ford L E 1982 Internal viscoelastic loading in cat papillary muscle *Biophys. J.* **40** 109–20

de Tombe P and ter Keurs H E 1992 An internal viscous element limits unloaded velocity of sarcomere shortening in rat myocardium *J. Physiol.* **454** 619–42

Fearn L A, Bartoo M L, Myers J A and Polack G H 1993 An optical fiber transducer for single myofibril force measurement *IEEE Trans. Biomed. Eng.* **40** 1127–32

Freiburg A *et al* 2000 Series of exon-skipping events in the elastic spring region of titin as the structural basis for myofibrillar elastic diversity *Circ. Res.* **86** 1114–21

Fung Y C 1993 *Biomechanics: Mechanical Properties of Living Tissues* (New York: Springer)

Gao M, Lu H and Schulten K 2002 Unfolding of titin domains studied by molecular dynamics simulations *J. Muscle Res. Cell Motil.* **23** 513–21

Golenhofen N, Arbeiter A, Koob R and Drenckhahn D 2002 Ischemia-induced association of the stress protein alpha B-crystallin with I-band portion of cardiac titin *J. Mol. Cell. Cardiol.* **34** 309–19

Granzier H, Kellermayer M, Helmes M and Trombitas K 1997 Titin elasticity and mechanism of passive force development in rat cardiac myocytes probed by thin-filament extraction *Biophys. J.* **73** 2043–53

Granzier H and Labeit S 2004 The giant protein titin: a major player in myocardial mechanics, signaling, and disease *Circ. Res.* **94** 284–95

Higuchi H 1996 Viscoelasticity and function of connectin/titin filaments in skinned muscle fibers *Adv. Biophys.* **33** 159–71

Higuchi H, Nakauchi Y, Maruyama K and Fujime S 1993 Characterization of β-connectin (titin 2) from striated muscle by dynamic light scattering *Biophys. J.* **65** 1906–15

Kellermayer M S, Smith S B, Bustamante C and Granzier H L 2001 Mechanical fatigue in repetitively stretched single molecules of titin *Biophys. J.* **80** 852–63

Kulke M, Fujita-Becker S, Rostkova E, Neagoe C, Labeit D, Manstein D J, Gautel M and Linke W A 2001 Interaction between PEVK-titin and actin filaments: origin of a viscous force component in cardiac myofibrils *Circ. Res.* **89** 874–81

Labeit S and Kolmerer B 1995 Titins, giant proteins in charge of muscle ultrastructure and elasticity *Science* **270** 293–6

Li H, Linke W A, Oberhauser A F, Carrion-Vazquez M, Kerkvliet J G, Lu H, Marszalek P E and Fernandez J M 2002 Reverse engineering of the giant muscle protein titin *Nature* **418** 998–1002

Linke W A, Bartoo M L, Ivemeyer M and Pollack G H 1996a Limits of titin extension in single cardiac myofibrils *J. Muscle Res. Cell Motil.* **17** 425–38

Linke W A, Ivemeyer M, Olivieri N, Kolmerer B, Rüegg J C and Labeit S 1996b Towards a molecular understanding of the elasticity of titin *J. Mol. Biol.* **261** 62–71

Linke W A and Fernandez J M 2002 Cardiac titin: molecular basis of elasticity and cellular contribution to elastic and viscous stiffness components in myocardium *J. Muscle Res. Cell Motil.* **23** 483–97

Linke W A, Ivemeyer M, Labeit S, Hinssen H, Rüegg J C and Gautel M 1997 Actin–titin interaction in cardiac myofibrils: probing a physiological role *Biophys. J.* **73** 905–19

Linke W A, Kulke M, Li H, Fujita-Becker S, Neagoe C, Manstein D J, Gautel M and Fernandez J M 2002 PEVK domain of titin: an entropic spring with actin-binding properties *J. Struct. Biol.* **137** 194–205

Linke W A, Stockmeier M R, Ivemeyer M, Hosser H and Mundel P 1998 Characterizing titin's I-band Ig domain region as an entropic spring *J. Cell Sci.* **111** 1567–74

Liversage A D, Holmes D, Knight P J, Tskhovrebova L and Trinick J 2001 Titin and the sarcomere symmetry paradox *J. Mol. Biol.* **305** 401–9

Marko J F and Siggia E D 1995 Stretching DNA *Macromolecules* **28** 8759–70

Marszalek P E, Lu H, Li H, Carrion-Vazquez M, Oberhauser A F, Schulten K and Fernandez J M 1999 Mechanical unfolding intermediates in titin molecules *Nature* **402** 100–3

Miller M K, Granzier H, Ehler E and Gregorio C C 2004 The sensitive giant: the role of titin-based stretch sensing complexes in the heart *Trends Cell Biol.* **14** 119–26

Minajeva A, Kulke M, Fernandez J M and Linke W A 2001 Unfolding of titin domains explains the viscoelastic behavior of skeletal myofibrils *Biophys. J.* **80** 1442–51

Minajeva A, Neagoe C, Kulke M and Linke W A 2002 Titin-based contribution to shortening velocity of rabbit skeletal myofibrils *J. Physiol.* **540** 177–88

Mutungi G and Ranatunga K W 1996 The viscous, viscoelastic and elastic characteristics of resting fast and slow mammalian (rat) muscle fibres *J. Physiol.* **496** 827–36

Neagoe C, Opitz C A, Makarenko I and Linke W A 2003 Gigantic variety: expression patterns of titin isoforms in striated muscles and consequences for myofibrillar passive stiffness *J. Muscle Res. Cell Motil.* **24** 175–89

Noble M I 1977 The diastolic viscous properties of cat papillary muscle *Circ. Res.* **40** 288–92

Oberhauser A F, Marszalek P E, Erickson H P and Fernandez J M 1998 The molecular elasticity of the extracellular matrix protein tenascin *Nature* **393** 181–5

Opitz C A, Kulke M, Leake M C, Neagoe C, Hinssen H, Hajjar R J and Linke W A 2003 Damped elastic recoil of the titin spring in myofibrils of human myocardium *Proc. Natl Acad. Sci. USA* **100** 12688–93

Rief M, Gautel M, Oesterhelt F, Fernandez J M and Gaub H E 1997 Reversible unfolding of individual titin immunoglobulin domains by AFM *Science* **276** 1109–12

Rief M, Fernandez J M and Gaub H E 1998 Elastically coupled two-level systems as a model for biopolymer extensibility *Phys. Rev. Lett.* **81** 4764–7

Trombitas K, Wu Y, McNabb M, Greaser M, Kellermayer M S, Labeit S and Granzier H 2003 Molecular basis of passive stress relaxation in human soleus fibers: assessment of the role of immunoglobulin-like domain unfolding *Biophys. J.* **85** 3142–53

Tskhovrebova L and Trinick J 2003 Titin: properties and family relationships *Nat. Rev. Mol. Cell Biol.* **4** 679–89

Tskhovrebova L, Trinick J, Sleep J A and Simmons R M 1997 Elasticity and unfolding of single molecules of the giant muscle protein titin *Nature* **387** 308–12

Wang K, McCarter R, Wright R, Beverly J and Ramirez-Mitchell R 1993 Viscoelasticity of the sarcomere matrix of skeletal muscles. The titin-myosin composite filament is a dual-stage molecular spring *Biophys. J.* **64** 1161–77

Watanabe K, Nair P, Labeit D, Kellermayer M S, Greaser M, Labeit S and Granzier H 2002 Molecular mechanics of cardiac titin's PEVK and N2B spring elements *J. Biol. Chem.* **277** 11549–58